

Precise ^{40}Ar – ^{39}Ar ages from the metamorphic sole rocks of the Tauride Belt Ophiolites, southern Turkey: implications for the rapid cooling history

ÖMER FARUK ÇELİK*, MICHEL DELALOYE† & GILBERT FERAUD‡

*Kocaeli Üniversitesi, Jeoloji Mühendisliği Bölümü, 41150 Kocaeli, Turkey

†University of Geneva, Department of Mineralogy, 1205 Geneva 4, Switzerland

‡UMR 6526 Géosciences Azur, CNRS-UNSA, O6108 Nice cedex 02, France

(Received 14 December 2004; accepted 22 August 2005)

Abstract – The Tauride Belt Ophiolites in southern Turkey are located on both sides of the E–W-trending, Mesozoic Tauride carbonate platform. They comprise the Lycian, Antalya, Beyşehir, Mersin, Alihoca and Pozantı-Karsantı ophiolites from west to east. Each ophiolite has a metamorphic rock unit either at the base of the peridotites or in the mélange units. The metamorphic sole rocks generally consist of amphibolite at the top and near the contact with the overlying tectonized harzburgite of the ophiolites, and mica schists mostly at the base, near the tectonic contact with the underlying ophiolitic mélange. ^{40}Ar – ^{39}Ar measurements from the metamorphic sole rocks of the Lycian, Antalya and Beyşehir ophiolites are the first precise ages dating intra-oceanic thrusting and the cooling age history during the closure of the Neotethyan Ocean. Amphiboles and white micas from the metamorphic sole rocks of the ophiolites yielded ^{40}Ar – ^{39}Ar ages between 90.7 ± 0.5 Ma and 93.8 ± 1.7 Ma and between 91.2 ± 2.3 Ma and 93.6 ± 0.8 Ma, respectively. Hornblende plateau ages from the amphibolites of the Lycian ophiolites (near Köyceğiz) agree with those of Antalya, indicating that they were metamorphosed simultaneously in the Neotethyan Ocean. The white micas display plateau ages concordant with the amphiboles from the same units in Köyceğiz and Yeşilova (Lycian ophiolites) and from the Pozantı-Karsantı ophiolite, suggesting that the metamorphic sole rocks were rapidly cooled after their generation.

Keywords: geochronology, ophiolite, East Mediterranean, Neotethys, Turkey.

1. Introduction

The Tauride Belt in southern Turkey is one of the best regions to observe Cretaceous ophiolites in the Alpine–Himalayan mountain system. Ophiolites of the Tauride Belt are remnants of the Mesozoic Neotethyan Ocean in the Eastern Mediterranean. The Tauride Belt Ophiolites (Fig. 1) present many questions concerning their age, emplacement mechanisms, the tectonic setting of formation and their root zones. Ricou, Argriadis & Marcoux (1975) suggested that all of the Cretaceous ophiolites were thrust from a single Tethyan ocean basin, located to the north of the Tauride carbonate platform, during Late Cretaceous–Early Tertiary times. Robertson & Woodcock (1980) and Şengör & Yılmaz (1981), on the other hand, suggested a southern and a multi-armed northern branch of the Neotethyan Ocean. They proposed that the Antalya ophiolite was derived from a southern branch of the Neotethyan Ocean basin while the Lycian, Beyşehir, Mersin, Alihoca and Pozantı-Karsantı ophiolites were derived from a northern branch of the Neotethyan Ocean basin.

Most of the ophiolites worldwide have metamorphic rocks at their base, which is very useful for their

interpretation, because the mineralogy and texture can be used to understand their metamorphic and deformational history. For this reason, many geologists have focused their attention on these rocks to interpret intra-oceanic thrusting and emplacement of the ophiolites. Previous geochronological studies on the metamorphic rocks associated with the Tauride Ophiolites focused on the metamorphic soles and their ages, most of which were measured using the K–Ar method. For instance, Thuizat *et al.* (1981) analysed two amphiboles from amphibolites (98 ± 4 Ma and 102 ± 4 Ma) and two micas from mica schist (91 ± 3 Ma and 93 ± 3 Ma) to date the metamorphic sole rocks of Lycian ophiolites. They obtained ages of 93 ± 3 Ma (amphibole) and 84 ± 3 Ma (plagioclase) from an amphibolite of the Beyşehir ophiolite. The same authors analysed amphibole from amphibolites and obtained ages of 98 ± 4 Ma and 95 ± 4 Ma for the ophiolites of Mersin and Pozantı-Karsantı, respectively. They also used the K–Ar method to date one garnet-amphibolite (Antalya ophiolite) at 94 ± 4 Ma (1σ) (hornblende) and 102.7 ± 7 Ma (plagioclase) and interpreted these as cooling ages. The same authors reported metamorphic ages for the whole Tauride Belt to be close to 95 Ma. Yılmaz & Maxwell (1982, 1984) measured three amphibolite samples from the Antalya ophiolite

* Author for correspondence: fcelik@kou.edu.tr

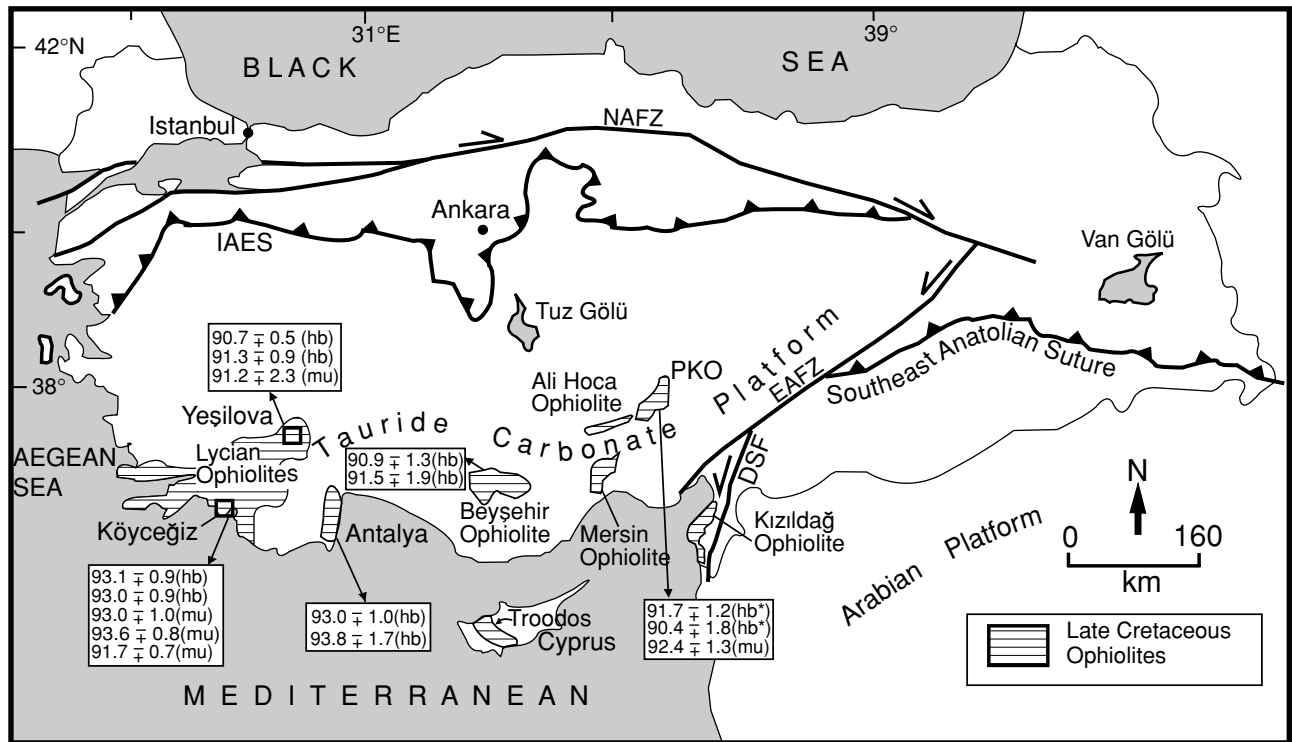


Figure 1. Generalized tectonic map of Turkey summarizing ^{40}Ar - ^{39}Ar geochronological data from the metamorphic rocks of the Tauride Belt Ophiolites. hb – hornblende; mu – muscovite (white mica), IAES – Izmir-Ankara-Erzincan Suture Zone, NAFZ – North Anatolian Fault Zone, EAFZ – East Anatolian Fault Zone, DSF – Dead Sea Fault, PKO – Pozantı-Karsantı ophiolite. Asterisk indicates reference: Dilek *et al.* (1999).

and obtained scattered K–Ar ages between 73.7 ± 1.1 and 78.5 ± 1.7 Ma (2σ) and interpreted these ages as Late Cretaceous metamorphic ages. Parlak, Delaloye & Bingöl (1995) reported K–Ar ages ranging from 77.1 ± 1.8 to 271.3 ± 7.1 on the amphibolites of the Mersin ophiolite.

^{40}Ar - ^{39}Ar geochronology results were obtained by Dilek *et al.* (1999) on amphibolite samples from the eastern part of the Tauride Belt Ophiolites (Mersin, Alihoca and Pozantı-Karsantı ophiolites). They presented plateau ages of 91.3 ± 0.4 and 93.8 ± 0.5 Ma for two amphibolites from the Mersin ophiolite. These ages were interpreted as cooling ages. The Alihoca ophiolite yielded an age of 90.6 ± 0.9 Ma on an amphibolite (hornblende), and exhibited an age of 90.8 ± 0.6 Ma on one dyke sample (hornblende). In the Mersin ophiolite, Parlak & Delaloye (1999) calculated a weighted mean ^{40}Ar - ^{39}Ar age of amphibolites (hornblende) at 92.6 ± 0.2 Ma (2σ) and interpreted this as the age of the intra-oceanic thrusting, during which sub-ophiolitic metamorphic sole rocks were developed.

Precise age constraints on the western (Lycian and Antalya ophiolites) and middle (Beyşehir ophiolite) Tauride Belt Ophiolites are lacking. Here, we report ^{40}Ar - ^{39}Ar age data on the ophiolites of Lycian, Antalya, Beyşehir and Pozantı-Karsantı, in order to constrain intra-oceanic thrusting and the cooling age history in the Neotethyan Ocean.

2. Regional geology

The Tauride Belt consists of a succession of nappe systems composed mainly of Palaeozoic and Early Mesozoic platform carbonates, volcano-sedimentary and epiclastic rocks, Cretaceous ophiolites, Late Cretaceous and younger post-collisional sediments and volcanic rocks (e.g. Özgül, 1976).

The Tauride ophiolitic massifs tectonically overlie the Tauride carbonate platform as dispersed slices and comprise three distinct structural elements. These are (1) an ophiolitic mélangé, (2) a metamorphic sole and (3) ultramafic and mafic rocks, which consist mainly of serpentinized peridotites, mafic-ultramafic cumulates and gabbros. Sheeted dykes and extrusive rocks are commonly missing (Juteau, 1980; Whitechurch, Juteau & Montigny, 1984; Dilek & Moores, 1990; Dilek *et al.* 1999).

The ophiolitic mélangés along the Tauride Belt include most or all of the units of an ophiolite; serpentinite, peridotite, gabbro, basalt, chert, radiolarites, pelagic sediments and fragments of the ophiolite-related metamorphic rocks occurring as blocks within the mélangé (Collins & Robertson, 1997; Parlak & Robertson, 2004). The ophiolitic mélangé is tectonically overlain by the metamorphic sole rocks that exhibit amphibolite facies close to the hanging peridotite contact and greenschist facies downward.

The ophiolites and the related metamorphic sole rocks have been extensively cut by numerous low-K mafic dyke swarms. However, these dykes do not cut the mélangé units or the platform carbonates, indicating that they were injected both into the metamorphic sole rocks and the ophiolites in an oceanic environment. In addition, the dolerite and gabbro dykes, which cross-cut the metamorphic sole rocks, show no indication of ductile deformation such as folding, which is common in the metamorphic sole rocks at the base of ophiolites (Çelik & Delaloye, 2003). This may indicate that the dyke injections into the metamorphic sole rocks were generated after the deformation phase.

To the west (e.g. the Lycian ophiolites), the general sense of displacement is NW–SE, as inferred from common mineral alignments of amphiboles in the amphibolites and intra-folial asymmetrical folds (Çelik & Delaloye, 2003). The same orientation was also reported in Lycian ophiolites by Collins & Robertson (1998, 2003). The Late Cretaceous Beyşehir ophiolite was initially obducted southward onto the Tauride carbonate platform, then in Late Eocene times it thrust further southeastward, together with the underlying Mesozoic platform carbonates (Andrew & Robertson, 2002). The Mersin ophiolite and related units were thrust southward over the Tauride carbonate platform from a northerly Neotethyan oceanic basin (Parlak & Robertson, 2004). There is kinematic evidence that the Pozanti-Karsanti ophiolite was also emplaced southward onto the Tauride carbonate platform in Late Cretaceous times (Polat & Casey, 1995).

2.a. Metamorphic sole rocks

The metamorphic sole rocks were observed across most of the Tauride Belt Ophiolites. They are tectonically located between the harzburgite tectonites and the mélangé below. The contact relationship between harzburgite tectonites and the sole rocks is generally defined by a 3–5 m thick, strongly sheared serpentized mantle tectonite. The metamorphic sole rocks at the base of the peridotites show highly folded and faulted structures, and therefore their actual thickness cannot be precisely defined. Nevertheless, rough thickness estimates indicate that the metamorphic sole rocks along the whole Tauride Belt Ophiolites never exceed 500 m. The metamorphic soles located at the base of the peridotites display an inverted metamorphic gradient from amphibolite-facies rocks, downward into greenschist-facies rocks and then into unmetamorphosed mélangé. The metamorphic sole rocks of Lycian and Pozanti-Karsanti ophiolites are among the best examples in which to study inverted metamorphic gradients. The metamorphic sole consists of garnet or pyroxene amphibolite in its upper part that

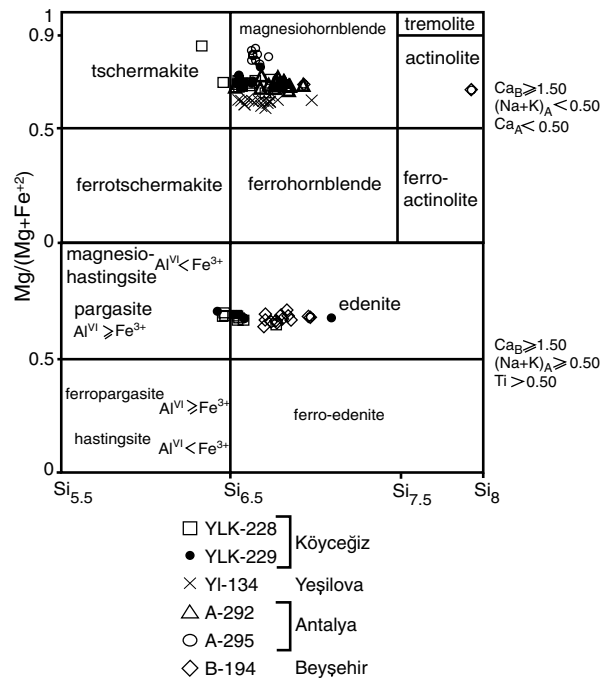


Figure 2. Chemical composition of amphiboles in amphibolites of the Köyceğiz, the Yeşilova, the Antalya and the Beyşehir ophiolites, after Leake *et al.* (1997).

changes gradually into epidote–amphibolite toward its base. The lower part of the metamorphic sole is composed of kyanite and garnet-bearing mica schist, mica schist, quartzite and marble. These rocks mainly show granoblastic, nematoblastic, porphyroblastic and lepidoblastic textures (Çelik & Delaloye, 2003).

Amphiboles from the amphibolites that we used for ^{40}Ar – ^{39}Ar geochronology are calcic amphibole in composition. They are represented by tschermakite, magnesiohornblende, actinolite, pargasite and edenite (Fig. 2). White micas in the mica schist of the Tauride Belt Ophiolites are generally represented by phengite. Mineral analyses were performed on a Cameca SX50 electron microprobe at University of Lausanne equipped with wavelength dispersive spectrometry. Operating conditions were 15 kV accelerating voltage and 15–30 nA sample current. Counting times of 10–30 s were applied. The complete dataset was published in Çelik (2002); a selection of the analyses is given here (Tables 1, 2).

Protoliths of the amphibolite rocks along the Tauride Belt Ophiolites are mostly basalts. Çelik & Delaloye (2003) indicated that the amphibolites display three different Rare Earth Element (REE) patterns which are represented by compositions corresponding to ocean island basalt (OIB), island arc tholeiite (IAT) and mid-ocean ridge basalt (MORB). The results show that there is not a unique protolith for the amphibolites (Çelik & Delaloye, 2002, 2003).

Table 1 Representative mineral compositions of the metamorphic sole rocks from the Tauride Belt Ophiolites (amphiboles from amphibolites)

Sample	YLK228-3	YLK228-4	YLK228-5	YLK229-1	YLK229-2	YLK229-3	YL134-2	YL134-3	YL134-4	A292-3	A292-4	A292-5	A295-6	A295-7	A295-9	B194-2	B194-3	B194-4
SiO ₂	45.91	43.89	44.88	45.75	44.56	45.44	44.83	45.98	44.33	46.48	47.5	47.69	46.63	46.58	46.97	46.16	47.31	47.03
TiO ₂	0.84	0.91	0.98	0.94	0.94	0.94	0.71	0.67	0.77	1.17	1.04	1.08	0.37	0.44	0.45	1.4	1.32	1.28
Al ₂ O ₃	12.08	12.89	13.02	12.58	13.19	12.58	11.66	10.32	11.99	10.31	9.51	9.77	13.12	13.41	13.65	9.95	8.86	9.95
Fe ₂ O ₃ (c)	1.28	9.66	2.58	1.55	2.89	1.72	1.79	2.23	1.74	3.6	1.6	0.85	2.58	0.83	1.45	1.65	2.16	0.54
FeO(c)	10.59	3.99	9.8	10.47	9.44	10.15	12.92	12.21	12.64	9.48	10.83	11.61	5.36	7.02	6.16	10.77	10.24	11.45
MnO	0.32	0.34	0.34	0.25	0.31	0.23	0.18	0.26	0.23	0.24	0.23	0.17	0.21	0.19	0.21	0.18	0.17	0.2
MgO	12.81	13.05	12.59	12.75	12.74	12.87	11.45	12.11	11.39	13.42	13.61	13.29	15.12	14.78	14.94	13.52	13.97	13.44
CaO	12.15	10.75	11.94	12.02	12.13	12.05	12.45	12.34	12.26	12.21	12.38	12.39	12.08	12.25	12	11.93	11.85	11.95
Na ₂ O	1.73	1.58	1.85	1.74	1.7	1.71	1.53	1.46	1.6	1.45	1.49	1.44	1.63	1.93	1.9	1.98	1.82	1.95
K ₂ O	0.57	0.72	0.79	0.85	0.86	0.86	0.51	0.42	0.69	0.36	0.34	0.34	0.38	0.31	0.37	0.69	0.55	0.64
F	0.07	0.02	0.06	0.07	0.05	0	0.02	0.07	0.05	0.03	0	0	0	0	0	0	0	0
H ₂ O(c)	2.04	2.07	2.04	2.05	2.05	2.08	2.03	2.01	2.01	2.07	2.08	2.08	2.11	2.11	2.12	2.06	2.07	2.07
Total	100.36	99.86	100.87	100.98	100.85	100.63	100.08	100.06	99.68	100.82	100.61	100.73	99.59	99.86	100.23	100.29	100.33	100.49
Si	6.635	6.332	6.471	6.578	6.428	6.555	6.587	6.731	6.543	6.687	6.843	6.864	6.625	6.624	6.631	6.705	6.841	6.801
Ti	0.091	0.099	0.107	0.101	0.102	0.102	0.079	0.074	0.085	0.126	0.112	0.117	0.039	0.047	0.048	0.153	0.144	0.139
Al ^{IV}	1.365	1.668	1.529	1.422	1.572	1.445	1.413	1.269	1.457	1.313	1.157	1.136	1.375	1.376	1.369	1.295	1.159	1.199
Al ^{VI}	0.692	0.524	0.684	0.71	0.67	0.693	0.606	0.512	0.628	0.436	0.458	0.522	0.821	0.872	0.903	0.408	0.351	0.496
Fe ³⁺	0.139	1.049	0.28	0.167	0.314	0.186	0.198	0.245	0.193	0.39	0.174	0.092	0.276	0.089	0.154	0.18	0.235	0.059
Fe ²⁺	1.28	0.481	1.182	1.259	1.139	1.225	1.587	1.495	1.56	1.14	1.305	1.398	0.637	0.835	0.727	1.308	1.238	1.384
Mn ²⁺	0.04	0.042	0.042	0.03	0.037	0.028	0.023	0.033	0.029	0.029	0.028	0.021	0.025	0.023	0.025	0.022	0.021	0.024
Mg	2.759	2.806	2.705	2.732	2.738	2.766	2.507	2.642	2.505	2.879	2.923	2.85	3.201	3.134	3.143	2.928	3.011	2.897
Ca	1.881	1.662	1.845	1.851	1.875	1.862	1.96	1.935	1.939	1.882	1.911	1.911	1.84	1.866	1.816	1.857	1.836	1.851
Na	0.486	0.441	0.517	0.484	0.477	0.478	0.435	0.415	0.457	0.405	0.417	0.403	0.45	0.532	0.519	0.556	0.511	0.546
K	0.104	0.132	0.145	0.156	0.159	0.159	0.096	0.078	0.131	0.067	0.062	0.063	0.069	0.056	0.066	0.128	0.102	0.118
F	0.034	0.009	0.029	0.033	0.022	0	0.008	0.034	0.023	0.014	0	0	0	0	0	0	0	0
Cl	0	0.003	0.005	0.001	0.002	0	0	0	0	0.004	0.001	0.002	0.002	0.002	0.007	0	0	0
OH	1.966	1.988	1.966	1.967	1.976	2	1.992	1.966	1.977	1.982	1.999	1.998	1.998	1.997	1.993	2	2	2
X _{Mg}	0.683	0.854	0.696	0.685	0.706	0.693	0.612	0.639	0.616	0.716	0.691	0.671	0.834	0.79	0.812	0.691	0.709	0.677

YLK – Lycian ophiolites (Köyceğiz region); YL – Lycian ophiolites (Yeşilova region); A – Antalya ophiolite; B – Beyşehir ophiolite.

Table 2 Representative mineral compositions of the metamorphic sole rocks from the Tauride Belt Ophiolites (micas from mica schists)

Sample	YLK253-1	YLK253-2	YLK253-3	YLK253-4	YLK253-5	YLK253-6	YLK253-7	YL90-1	YL90-2	YL90-3	YL90-4	PK20-4	PK20-18	PK20-19	PK20-20	PK20-21	PK20-22	PK20-23
SiO ₂	47.37	47.58	48.17	47.81	47.5	47.02	47.8	47.08	46.83	47.01	47.11	47.12	47.76	47.42	47.21	47.03	47.27	47.22
TiO ₂	0.86	0.65	0.68	0.69	0.74	0.73	0.89	0.51	0.42	0.4	0.47	1.06	1.25	1.36	1.12	1.02	1.07	1.21
Al ₂ O ₃	32.38	32.42	32.78	32.1	32.38	31.78	32.52	33.28	33.06	33.21	32.9	32.07	32.48	32.23	32.84	32.76	32.59	32.78
Cr ₂ O ₃	0.05	0	0	0	0	0	0.17	0.14	0.04	0	0	0	0.05	0.06	0	0.25	0.01	0
FeO	3.45	3.59	3.51	3.73	3.47	3.49	3.49	4.11	4.28	4.23	3.98	3.59	3.68	3.78	3.82	4.15	3.82	4.18
MnO	0.00	0.15	0.1	0.04	0	0.06	0.12	0	0.15	0	0.11	0.12	0	0.01	0.09	0	0	0.11
MgO	1.56	1.86	1.68	1.87	1.64	1.7	1.82	1.24	1.25	1.24	1.29	1.74	1.63	1.83	1.54	1.75	1.73	1.64
CaO	0.01	0.03	0.01	0.02	0	0.01	0.05	0.01	0	0.03	0	0.05	0.01	0.01	0.03	0.03	0.01	0.01
Na ₂ O	1.58	1.78	1.67	1.66	1.64	1.66	1.59	0.82	0.9	0.87	0.78	0.96	0.92	0.95	1.01	0.97	0.95	0.96
K ₂ O	6.27	6.26	5.84	5.96	5.82	7.76	6.35	6.85	7.28	6.88	6.86	6.24	6.2	6.25	6.43	6.29	6.28	6.35
BaO	0.18	0.11	0.16	0.17	0.19	0.13	0.2	0.19	0.14	0.23	0.17	0.38	0.37	0.41	0.34	0.38	0.4	0.41
SrO	0.29	0	0.54	0.54	0.53	0.55	0.57	0.55	0.48	0.28	0.56	0.54	0.54	0.5	0.55	0.53	0	0.11
Cl	0.00	0.01	0.01	0	0	0	0	0.01	0	0.01	0	0.01	0	0	0	0.01	0	0.01
H ₂ O(c)	4.48	4.5	4.54	4.5	4.48	4.46	4.54	4.49	4.48	4.47	4.47	4.46	4.52	4.5	4.5	4.5	4.49	4.51
Total	98.48	98.93	99.68	99.09	98.39	99.35	100.11	99.29	99.31	98.88	98.69	98.34	99.4	99.3	99.48	99.67	98.61	99.49
Si	6.342	6.338	6.362	6.369	6.357	6.317	6.318	6.285	6.274	6.297	6.322	6.334	6.341	6.316	6.284	6.258	6.316	6.279
Ti	0.087	0.066	0.068	0.069	0.074	0.074	0.089	0.051	0.042	0.041	0.047	0.108	0.124	0.136	0.113	0.103	0.108	0.121
Al ^{IV}	1.658	1.662	1.638	1.631	1.643	1.683	1.682	1.715	1.726	1.703	1.678	1.666	1.659	1.684	1.716	1.742	1.684	1.721
Al ^{VI}	3.451	3.429	3.466	3.408	3.465	3.348	3.385	3.521	3.494	3.539	3.524	3.415	3.424	3.375	3.435	3.396	3.449	3.416
Cr	0.005	0	0	0	0	0	0.017	0.015	0.005	0	0	0	0.005	0.006	0	0.026	0.001	0
Fe ²⁺	0.386	0.4	0.387	0.416	0.388	0.393	0.386	0.459	0.48	0.474	0.446	0.403	0.408	0.421	0.425	0.462	0.427	0.465
Mg	0.31	0.369	0.33	0.372	0.327	0.341	0.36	0.248	0.25	0.248	0.258	0.349	0.323	0.363	0.305	0.347	0.344	0.324
Ca	0.002	0.004	0.001	0.003	0	0.001	0.007	0.002	0	0.004	0	0.007	0.001	0.001	0.004	0.004	0.001	0.001
Na	0.41	0.461	0.427	0.428	0.425	0.432	0.408	0.212	0.233	0.227	0.204	0.25	0.237	0.245	0.26	0.249	0.246	0.247
K	1.071	1.063	0.983	1.013	0.993	1.33	1.07	1.167	1.244	1.176	1.174	1.07	1.05	1.062	1.093	1.067	1.071	1.077
Ba	0.009	0.006	0.008	0.009	0.01	0.007	0.01	0.01	0.007	0.012	0.009	0.02	0.019	0.021	0.018	0.02	0.021	0.021
Sr	0.022	0	0.042	0.042	0.041	0.042	0.043	0.043	0.038	0.022	0.044	0.042	0.042	0.039	0.042	0.041	0	0.009
OH	4	3.998	3.998	4	4	3.999	4	3.998	4	3.997	4	3.998	4	4	3.999	3.998	3.999	3.998
X _{Mg}	0.446	0.48	0.46	0.472	0.457	0.465	0.482	0.351	0.343	0.343	0.367	0.464	0.442	0.463	0.417	0.429	0.446	0.411

YLK – Lycian ophiolites (Köyceğiz region); YL – Lycian ophiolites (Yeşilova region); PK – Pozantı–Karsantı ophiolite.

3. Geochronology

3.a. Methodology

The ^{40}Ar – ^{39}Ar analyses were carried out at the Géosciences Azur laboratory in Nice. The extracted minerals were obtained by magnetic separation, heavy liquids and hand picking under a binocular microscope in order to produce high-purity mineral separates (> 99%). Samples were irradiated for 25 hours in the nuclear reactor at McMaster University in Hamilton, Canada, in position 5c. The total neutron flux during irradiation is 3.15×10^{18} n·cm $^{-2}$, with a maximum flux gradient estimated at $\pm 0.2\%$ in the volume where the samples were included.

The gas extraction was carried out by a 50 watt Synrad infrared CO $_2$ continuous laser, and the mass spectrometer was a VG 3600 working with a Daly detector system. Argon isotopes were typically on the order of 40–400 and 100–900 times the blank level, for the ^{40}Ar and ^{39}Ar , respectively. Corrections for neutron-induced reactions on ^{40}K and ^{40}Ca are: (^{40}Ar – ^{39}Ar) $_K = 0.0297$; (^{36}Ar – ^{37}Ar) $_{Ca} = 0.000279$; (^{39}Ar – ^{37}Ar) $_{Ca} = 0.000706$. All ages are calculated for FCs = 28.02 Ma (Renne *et al.* 1998). K decay constants are those of Steiger & Jaeger (1977). The criteria for defining plateau ages were the following: (1) at least 70% of released ^{39}Ar ; (2) at least three successive steps in the plateau and (3) the integrated age of the plateau should agree with each apparent age of the plateau within a 2σ confidence interval. Plateau ages are given at the 2σ level. Uncertainties on the apparent ages on each step are quoted at the 1σ level and do not include the uncertainties on the age of the monitor. The uncertainties on the ^{40}Ar */ ^{39}Ar $_K$ ratios of the monitor are included in the calculation of the plateau age uncertainty. Detailed ^{40}Ar – ^{39}Ar analytical data are given in Table 3.

3.a.1. Samples used for ^{40}Ar – ^{39}Ar geochronology

The metamorphic sole rocks from the ophiolites of Lycian (at Köyceğiz and Yeşilova) and Pozantı-Karsantı were sampled between the harzburgite tectonites and the mélangé. The metamorphic sole rocks of the Antalya and Beyşehir ophiolites could not be found at the base of the harzburgite tectonites, therefore they were collected from the mélangé. Analyses for the Köyceğiz amphibolite were performed on single crystals of amphibole about 0.45–0.9 mm (sample YLK-228) and 0.3–0.6 mm (sample YLK-229) in size. The vertical distance between the two analysed amphibolites is around 15 m to 20 m. A small cluster of small amphibole crystals was used for the Yeşilova unit: seven and eight single grains for the samples YL-103 and YL-134, respectively. The distance between the outcrops from which the two analysed amphibolite samples (YL-103 and YL-134) were taken is 6 km. ^{40}Ar – ^{39}Ar age analyses for the Antalya ophiolite were

performed on amphibolites of the Alakır Çay Mélangé. The amphiboles (A-292 and A-295) are single grains with a size of 1.3 to 0.6 mm and 1.1 to 0.5 mm, respectively. The samples were collected close to Sarıcık School (Çelik & Delaloye, 2003) and the distance between the outcrops is approximately 1 km. Those of the Beyşehir ophiolite were performed on small clusters of six to nine single grains of amphibole of about 0.3–0.9 mm for sample B-192 and 0.25–0.50 mm for sample B-194. The two samples are located only 20 m apart in the field. Three white mica samples (YLK-253 (0.45–0.63 mm in size), YLK-255 (0.35–0.7 mm in size) and YLK-266 (0.5–0.7 mm in size)) from the Köyceğiz mica schists, one white mica from the Yeşilova mica schist (YL-106; 0.45–0.6 mm in size) and one white mica from the Pozantı-Karsantı mica schist (PK-20; 0.45–0.6 mm in size) were also measured.

3.b. ^{40}Ar – ^{39}Ar results

3.b.1. Lycian ophiolites (Köyceğiz area)

The two amphibole single grains from the amphibolites (YLK-228 and YLK-229) yielded concordant plateau ages of 93.1 ± 0.9 Ma and 93.0 ± 0.9 Ma over more than 76% of the ^{39}Ar released (Fig. 3a, b). In both cases, the lower ages at low temperature are the result of cryptic alteration products (as shown by the significantly lower and variable $^{37}\text{Ar}_{Ca}/^{39}\text{Ar}_K$). In contrast, the plateau ages correspond to homogeneous $^{37}\text{Ar}_{Ca}/^{39}\text{Ar}_K$ ratios and are therefore interpreted as pure amphibole. Among the three analysed white micas from the Köyceğiz metamorphic sole rocks (mica schists), two samples displayed concordant plateau ages of 93.0 ± 1.0 (YLK-253) and 93.6 ± 0.8 Ma (YLK-266) (Fig. 3c, d) that are also concordant with the amphibole plateau ages. In the study area, nevertheless, white mica from the sample YLK-255 yielded a younger plateau age of 91.7 ± 0.7 Ma (Fig. 3e).

3.b.2. Lycian ophiolites (Yeşilova area)

Amphiboles from amphibolite samples (YL-103 and YL-134) display concordant plateau ages ranging between 90.7 ± 0.5 Ma and 91.3 ± 0.9 Ma (Fig. 4a, b). The white mica from the mica schist sample (YL-106), analysed by ^{40}Ar – ^{39}Ar , also exhibits a concordant age of 91.2 ± 2.3 Ma (over 90% of the total ^{39}Ar released) at 2σ level (Fig. 4c).

3.b.3. Antalya ophiolite (Alakır Çay Mélangé)

Samples A-292 (amphibolite) and A-295 (pyroxene–amphibolite) yielded plateau ages of 93.0 ± 1.0 Ma and 93.8 ± 1.7 Ma respectively (Fig. 5a, b). These plateau ages correspond to pure amphibole, as shown by flat $^{37}\text{Ar}_{Ca}/^{39}\text{Ar}_K$ ratio spectra.

Table 3. Detailed $^{40}\text{Ar}/^{39}\text{Ar}$ analytical data for the hornblendes and white micas

Step no.	Atmospheric contamination (%)	^{39}Ar (%)	$^{37}\text{Ar}_{\text{Ca}}/^{39}\text{Ar}_{\text{K}}$	$^{40}\text{Ar}^*/^{39}\text{Ar}_{\text{K}}$	Age (Ma)
YLK-228 (hornblende)					
1	47.321	7.68	0.951	7.538	84.0 ± 2.1
2	0.000	2.25	0.743	7.875	87.7 ± 7.2
3	0.000	1.72	1.725	7.742	86.2 ± 7.1
4	0.000	2.11	3.846	8.728	96.9 ± 6.8
5	2.693	5.62	6.858	8.360	92.1 ± 3.1
6	4.090	16.67	7.325	8.382	93.2 ± 1.0
7	1.614	23.75	7.267	8.429	93.7 ± 0.7
8	1.126	19.47	7.391	8.356	92.9 ± 0.7
9	0.773	13.26	8.085	8.356	92.9 ± 0.9
10	6.308	2.73	8.607	8.012	89.2 ± 4.7
Fusion	3.363	4.74	7.696	8.321	92.5 ± 2.8
					Integrated age = 92.2 ± 0.5
YLK-229 (hornblende)					
1	41.315	20.11	0.662	7.752	86.4 ± 0.8
2	17.741	3.42	3.946	8.560	95.2 ± 3.7
3	6.159	8.12	6.618	8.600	95.6 ± 1.6
4	1.940	28.67	7.312	8.359	93.0 ± 0.5
5	1.276	15.10	7.410	8.270	92.0 ± 1.1
6	0.698	17.56	7.411	8.309	92.5 ± 0.6
7	3.170	1.02	7.586	8.111	90.3 ± 11.8
Fusion	1.383	6.01	8.074	8.462	94.1 ± 2.3
					Integrated age = 91.8 ± 0.4
YLK-253 (muscovite)					
1	21.771	3.29	0.023	8.113	84.6 ± 6.0
2	13.869	2.55	0.026	8.027	83.7 ± 8.2
3	1.158	27.16	0.005	8.931	92.9 ± 0.6
4	0.194	13.28	0.000	9.075	94.4 ± 1.1
5	1.387	21.46	0.006	8.886	92.5 ± 1.0
6	0.143	8.81	0.000	8.937	93.0 ± 2.2
7	1.727	5.01	0.003	8.782	91.4 ± 3.2
Fusion	0.000	18.45	0.002	8.959	93.2 ± 1.1
					Integrated age = 92.5 ± 0.5
YLK-255 (muscovite)					
1	19.448	1.29	0.000	9.177	95.4 ± 9.5
2	53.723	1.09	0.000	8.749	91.7 ± 13.6
3	42.083	0.36	0.000	6.307	66.1 ± 32.2
4	66.803	1.81	0.027	7.389	77.2 ± 9.2
5	15.119	5.36	0.000	8.933	92.9 ± 3.3
6	2.747	4.16	0.033	8.799	91.6 ± 4.5
7	2.352	34.79	0.001	8.844	92.0 ± 0.3
8	3.466	13.29	0.000	8.706	90.6 ± 1.1
9	2.964	7.94	0.003	8.829	91.9 ± 1.1
10	6.213	12.31	0.006	8.814	91.7 ± 1.3
Fusion	3.027	17.62	0.007	8.804	91.6 ± 1.1
					Integrated age = 91.4 ± 0.5
YLK266 (muscovite)					
1	0.000	0.10	0.263	9.266	96.3 ± 146.8
2	3.718	1.71	0.010	10.316	106.9 ± 8.8
3	5.714	3.65	0.042	9.393	97.6 ± 3.0
4	0.000	2.80	0.002	9.260	96.2 ± 5.7
5	0.239	41.17	0.002	9.020	93.8 ± 0.4
6	0.000	7.72	0.007	9.148	95.1 ± 2.5
7	0.556	26.24	0.007	8.919	92.8 ± 0.7
Fusion	0.000	16.61	0.001	8.987	93.5 ± 0.9
					Integrated age = 94.0 ± 0.5
YL-103 (hornblende)					
1	88.325	0.42	12.498	8.929	99.1 ± 36.1
2	88.980	0.22	9.347	1.494	16.9 ± 78.5
3	56.994	0.69	7.779	4.319	48.6 ± 12.9
4	0.000	1.41	6.704	9.540	105.7 ± 11.2
5	0.000	6.25	6.461	8.600	95.5 ± 3.1
6	0.000	21.38	6.404	8.451	93.9 ± 0.9
7	4.844	17.30	6.341	8.095	90.0 ± 1.1
8	2.978	7.20	6.480	8.037	89.4 ± 2.5
9	6.251	15.19	6.225	7.788	86.7 ± 1.4
10	5.373	3.58	6.305	7.861	87.5 ± 4.7
11	8.383	4.48	6.231	7.575	84.4 ± 4.8
12	4.673	4.90	6.236	7.887	87.8 ± 4.2
Fusion	0.000	17.00	6.065	8.347	92.8 ± 1.0
					Integrated age = 90.5 ± 0.6

Table 3. Continued.

Step no.	Atmospheric contamination (%)	³⁹ Ar (%)	³⁷ Ar _{Ca} / ³⁹ Ar _K	⁴⁰ Ar*/ ³⁹ Ar _K	Age (Ma)
YL-134 (hornblende)					
1	76.074	2.76	1.359	8.700	96.7 ± 7.8
2	10.291	0.83	1.718	9.918	109.8 ± 17.5
3	20.065	1.16	4.931	8.167	90.9 ± 19.0
4	16.004	1.00	7.169	9.738	107.9 ± 17.2
5	38.665	1.17	6.945	11.877	130.7 ± 15.5
6	8.716	4.55	7.161	8.640	96.0 ± 4.0
7	10.296	26.69	7.523	8.319	92.5 ± 0.9
8	12.987	30.42	7.820	8.650	96.1 ± 1.0
9	0.000	3.96	7.373	9.328	103.4 ± 4.4
10	24.116	1.95	7.467	7.010	78.3 ± 7.7
Fusion	11.327	25.52	7.549	8.135	90.5 ± 0.7
					Integrated age = 94.3 ± 0.7
YL-106 (muscovite)					
1	36.101	3.02	0.136	5.819	61.1 ± 14.7
2	15.667	2.16	0.000	8.301	86.5 ± 18.2
3	52.967	2.86	0.000	8.799	91.6 ± 19.7
4	39.139	1.51	0.009	7.188	75.2 ± 25.8
5	3.125	66.22	0.004	8.842	92.0 ± 0.9
6	6.738	14.01	0.010	8.563	89.2 ± 4.1
Fusion	5.659	10.22	0.028	8.521	88.8 ± 6.7
					Integrated age = 90.0 ± 1.4
A-292 (hornblende)					
1	93.420	0.34	10.4	39.808	405.6 ± 68.1
2	107.606	0.04	7.25	-29.581	0.0 ± 0.0
3	95.910	0.08	11.2	32.398	336.7 ± 251.9
4	94.320	0.12	9.63	37.690	386.2 ± 166.3
5	84.610	0.52	14.5	5.262	59.2 ± 31.6
6	41.080	24.69	13.1	8.652	96.3 ± 1.1
7	5.755	53.35	13.0	8.234	91.7 ± 0.6
8	3.869	8.46	13.1	8.262	92.0 ± 2.2
9	10.000	5.86	13.4	7.933	88.4 ± 2.6
Fusion	10.490	6.55	13.2	7.770	86.7 ± 2.6
					Integrated age = 93.8 ± 0.7
A-295 (hornblende)					
1	86.762	0.44	9.402	17.310	187.6 ± 74.3
2	116.446	0.10	8.768	-17.521	0.0 ± 0.0
3	79.946	0.26	10.936	16.400	178.2 ± 95.7
4	23.449	0.15	14.315	17.934	194.0 ± 195.6
5	23.038	1.07	14.792	10.578	116.9 ± 31.2
6	63.212	1.47	17.432	5.041	56.7 ± 25.2
7	11.062	51.09	15.370	8.621	95.9 ± 0.8
8	2.511	5.46	14.988	8.154	90.8 ± 4.8
9	6.982	13.92	15.313	7.963	88.7 ± 4.0
10	0.460	10.16	15.404	8.519	94.8 ± 3.0
11	2.612	9.74	15.137	8.130	90.5 ± 3.0
12	0.000	0.79	15.561	9.883	109.5 ± 45.0
Fusion	0.000	5.35	15.546	8.929	99.2 ± 4.4
					Integrated age = 94.4 ± 1.2
B-192 (hornblende)					
1	58.097	11.08	11.817	7.863	87.7 ± 2.6
2	16.191	2.52	11.215	8.167	91.0 ± 8.6
3	12.074	4.26	12.120	7.885	87.9 ± 4.7
4	0.000	3.01	12.165	8.607	95.7 ± 6.4
5	6.766	28.85	11.992	8.236	91.7 ± 0.9
6	7.664	17.63	11.980	8.390	93.4 ± 1.1
7	6.998	15.31	12.041	8.189	91.2 ± 1.3
8	4.954	6.18	12.105	8.167	91.0 ± 3.1
Fusion	9.172	11.16	12.290	7.849	87.5 ± 1.6
					Integrated age = 90.9 ± 0.7
B-194 (hornblende)					
1	89.516	0.32	6.395	18.546	200.2 ± 70.2
2	96.149	0.05	16.085	13.639	149.4 ± 585.6
3	100.574	0.11	16.704	-0.825	0.0 ± 0.0
4	35.250	0.14	15.620	23.247	247.6 ± 165.9
5	61.431	0.14	15.690	6.177	69.2 ± 159.1
6	107.497	0.24	16.801	-3.597	0.0 ± 0.0
7	76.852	0.80	14.625	12.891	141.5 ± 42.0
8	45.074	1.08	11.901	9.689	107.4 ± 24.4
9	38.488	15.67	8.911	8.554	95.1 ± 2.2
10	29.451	31.75	10.018	8.208	91.4 ± 1.2

Table 3. Continued.

Step no.	Atmospheric contamination (%)	³⁹ Ar (%)	³⁷ Ar _{Ca} / ³⁹ Ar _K	⁴⁰ Ar*/ ³⁹ Ar _K	Age (Ma)
11	35.427	2.52	9.279	8.412	93.6 ± 10.3
12	13.660	2.29	9.328	8.447	93.9 ± 10.8
13	29.964	22.15	8.888	8.236	91.7 ± 1.0
14	29.759	7.82	8.975	8.014	89.2 ± 5.9
15	26.059	4.80	9.797	7.783	86.7 ± 6.6
16	21.751	9.16	9.735	7.998	89.1 ± 2.7
Fusion	54.528	0.94	10.123	5.176	58.1 ± 30.0
					Integrated age = 92.0 ± 1.2
PK-20 (muscovite)					
1	27.013	4.03	0.039	7.868	82.1 ± 5.0
2	0.000	1.88	0.000	9.788	101.6 ± 18.3
3	12.680	11.05	0.000	8.648	90.0 ± 1.1
4	2.956	3.70	0.026	9.355	97.2 ± 8.6
5	10.780	4.26	0.040	8.517	88.7 ± 4.2
6	2.508	27.57	0.003	8.950	93.1 ± 1.0
7	5.218	7.17	0.019	8.731	90.9 ± 3.5
Fusion	1.701	40.34	0.003	8.913	92.7 ± 0.7
					Integrated age = 92.1 ± 0.8

3.b.4. Beyşehir ophiolite

The small clusters of amphibole grains from amphibolite samples (B-192 and B-194) display equivalent plateau ages of 90.9 ± 1.3 and 91.5 ± 1.9 Ma, respectively (Fig. 6a, b).

3.b.5. Pozanti-Karsanti ophiolite

The white mica from the mica schist (PK-20) of the Pozanti-Karsanti metamorphic sole rocks was also analysed by ⁴⁰Ar–³⁹Ar method and yielded a plateau age of 92.4 ± 1.3 Ma (Fig. 7).

4. Discussion and comparison of radiometric age results

The overall ⁴⁰Ar–³⁹Ar plateau ages obtained on ophiolites from the five regions range between 90.7 ± 0.5 and 93.8 ± 1.7 Ma for the amphiboles, and between 91.2 ± 2.3 and 93.6 ± 0.8 Ma for the white micas.

The previous K–Ar ages (e.g. 95 Ma: Thuzat *et al.* 1981; 73–78 Ma: Yılmaz & Maxwell, 1982, 1984) are not consistent with our ⁴⁰Ar–³⁹Ar results, and an interpretation of these ages as a Late Cretaceous metamorphic age is not reasonable. The diffusion behaviour for radiogenic argon in amphibole structure during slow cooling or during thermal events subsequent to the original crystallization produces a broad scatter of K–Ar ages in K–Ar dating when compared to the ⁴⁰Ar–³⁹Ar method. When we compare our data with those previously obtained by some authors, we observe reasonably good correlation of age data. For instance, the white mica plateau age of 92.4 ± 1.3 Ma obtained from the Pozanti-Karsanti ophiolite is similar to those obtained from amphiboles (91.7 ± 1.2 (2σ) and 90.4 ± 1.8 Ma) by Dilek *et al.* (1999). Moreover, when we compare our age data with those (⁴⁰Ar–³⁹Ar as well) previously obtained by Dilek *et al.* (1999) and Parlak & Delaloye (1999) on amphibolite samples from the

eastern part of the Tauride ophiolites (Mersin, Alihoca and Pozanti-Karsanti ophiolites), we observe a general agreement of data.

Because of the clustering of ⁴⁰Ar–³⁹Ar plateau ages, we consider these data in the following discussion.

The closure temperature of amphibole in the ⁴⁰Ar–³⁹Ar system was estimated to be on the order of 500–550 °C for moderate cooling rates (Hanson & Gast, 1967; Harrison, 1981). Geothermometry on rocks from Köyceğiz indicate that the metamorphic temperature in the sole rocks was approximately 550 °C (Çelik, 2002; Çelik & Delaloye, 2004), based on the hornblende–plagioclase geothermometer of Holland & Blundy (1994) and the garnet–hornblende geothermometer of Graham & Powell (1984). This corresponds to the closure temperature of amphibole in the ⁴⁰Ar–³⁹Ar system and therefore 93.1 ± 0.6 Ma could be interpreted as approaching the metamorphic age of the amphibolites. The metamorphic temperature in the Yeşilova amphibolites was estimated to be 600–650 °C (Çelik & Delaloye, 2004), based on the hornblende–plagioclase geothermometer of Holland & Blundy (1994). These temperatures are higher than the closure temperature of amphiboles in the ⁴⁰Ar–³⁹Ar system. For this reason, 90.7 ± 0.5 Ma and 91.3 ± 0.9 Ma could be interpreted as cooling age of the metamorphic sole rocks. As the matrix of the Antalya and the Beyşehir mélange units are not metamorphic, the amphibolites could have been incorporated into the mélange units after the metamorphism. Although the metamorphic rocks of Beyşehir ophiolite are located in the mélange unit, we performed some geothermometer measurements on the amphibolite samples and deduced a metamorphic temperature of 550–600 °C (Çelik & Delaloye, 2006), based on the hornblende–plagioclase geothermometer of Holland & Blundy (1994). This temperature is close to the closure temperature of amphibole and therefore, the age of 91.1 ± 1.1 Ma may be interpreted as either a cooling age or as the metamorphic age of the amphibolites.

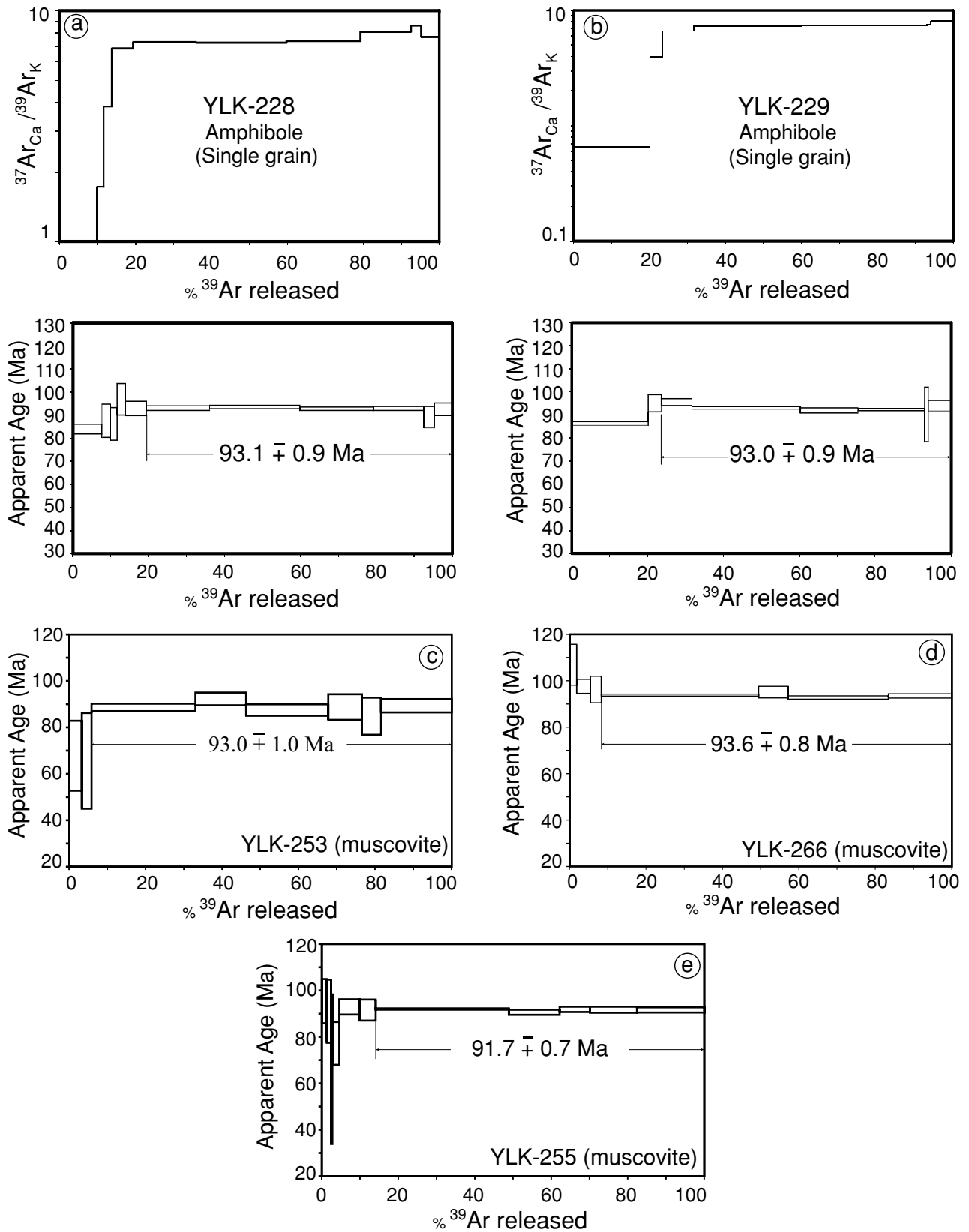


Figure 3. ^{40}Ar - ^{39}Ar ages and $^{37}\text{Ar}_{\text{Ca}}/^{39}\text{Ar}_{\text{K}}$ ratio spectra for hornblende (a, b) and white mica crystalloblasts (c, d, e) from the amphibolites and the mica schists of Köyceğiz region (Lycian ophiolites). All error boxes are at the 1σ level. Arrows show the steps included in the plateau age (given at the 2σ level).

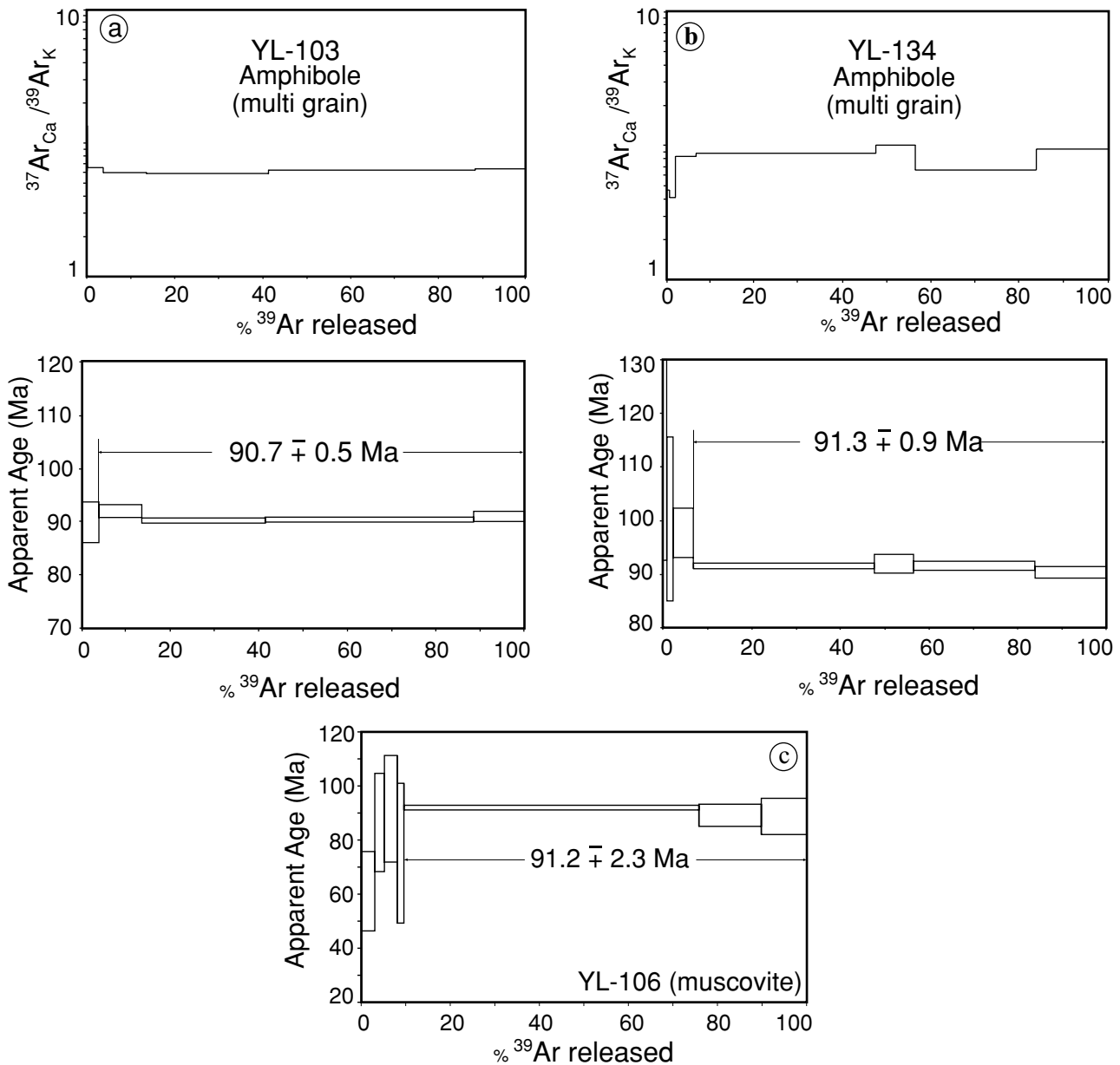


Figure 4. ^{40}Ar – ^{39}Ar ages and $^{37}\text{Ar}_{\text{Ca}}$ – $^{39}\text{Ar}_{\text{K}}$ ratio spectra for hornblende (a, b) and white mica crystalloblasts (c) from the amphibolites and the mica schists of Yeşilova region (Lycian ophiolites).

The plateau ages displayed by amphiboles from different rocks from the same unit are mostly concordant and may be slightly different from one unit to the other. For instance, the youngest amphibole ages are obtained in Yeşilova (90.7 ± 0.5 and 91.3 ± 0.9 Ma) and are may be distinct from those obtained in Köyceğiz (93.1 ± 0.9 and 93.0 ± 0.9 Ma). Another important observation concerns the white micas that display plateau ages concordant with the amphiboles from the same units, in Köyceğiz (93.0 ± 1.0 and 93.6 ± 0.8 Ma, but YLK-255 sample slightly younger) and Yeşilova (91.2 ± 2.3 Ma). Pozantı-Karsantı ophiolite also displays the same plateau ages between amphiboles (91.7 ± 1.2 and 90.4 ± 1.8 Ma; Dilek *et al.* 1999) and white mica

(92.4 ± 1.3 Ma). K–Ar blocking temperatures for white mica and amphibole are on the order of 350 and 500–550 °C, respectively and therefore, this suggests that the metamorphic sole rocks along the Tauride Belt Ophiolites were rapidly cooled after their generation.

We interpret the hornblende age as a metamorphic age for the Köyceğiz amphibolite. The oldest white mica age in the mica schists is 93.6 ± 0.8 Ma. Accordingly, the youngest hornblende age from the amphibolites could be as young as 92.8 Ma. In other words, the intra-oceanic thrusting age of the ophiolites must be older than 92.8 Ma. This interpretation is also consistent with our ^{40}Ar – ^{39}Ar data from the Köyceğiz amphibolites.

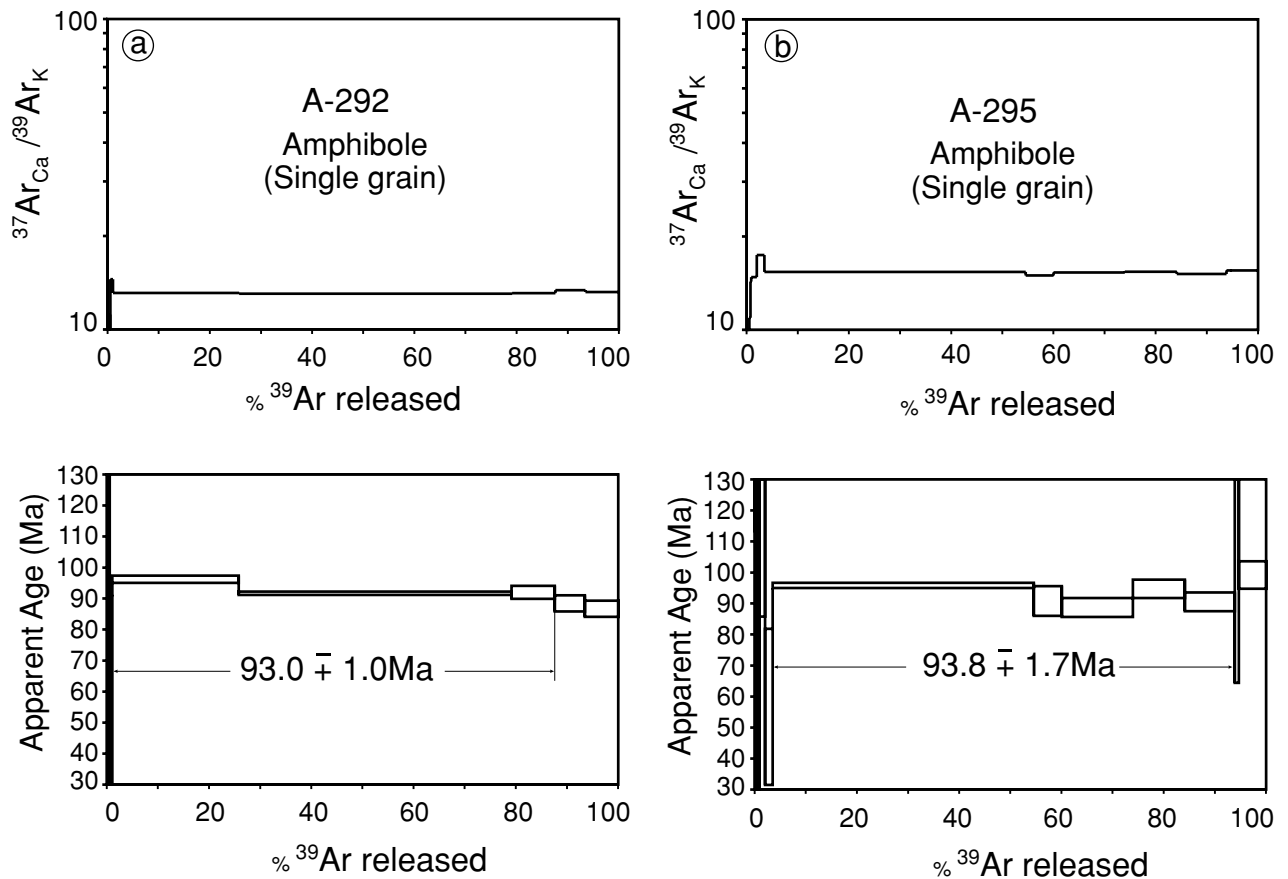


Figure 5. ^{40}Ar – ^{39}Ar ages and $^{37}\text{Ar}_{\text{Ca}}$ – $^{39}\text{Ar}_{\text{K}}$ ratio spectra for hornblende (a, b) from amphibolites of the Antalya ophiolite.

Robertson & Woodcock (1980) and Şengör & Yılmaz (1981) reported that while Antalya ophiolites were derived from a southern branch of the Neotethyan Ocean basin, the other Tauride Belt Ophiolites (e.g. Köyceğiz and Pozantı-Karsantı ophiolites) were derived from a multi-armed northern branch of the Neotethyan Ocean basin. However, according to our ^{40}Ar – ^{39}Ar data, the hornblende plateau ages from the amphibolites of Köyceğiz (93.1 ± 0.9 Ma and 93.0 ± 0.9 Ma) are equivalent to those of Antalya (93.0 ± 1.0 and 93.8 ± 1.7 Ma), indicating that they were metamorphosed simultaneously (probably in the same oceanic basin?) in the Neotethyan Ocean.

5. Proposed tectonic model

During the Jurassic to Early Cretaceous time interval, growth of oceanic crust was continuing in the southern and multi-armed northern branch of the Neotethyan Ocean (Şengör & Yılmaz, 1981). Extensive Late Jurassic to Early Cretaceous ocean island (OIB) or seamount type alkaline basaltic volcanic rocks that are intercalated with cherty limestone and radiolaria were reported in the Mersin ophiolite (Parlak, 1996). According to Smith, Hurley & Briden (1981), the

southern Atlantic Ocean began to open during the Early–Late Cretaceous. Thus the convergence between the Afro-Arabian and Eurasian plates began and, as a consequence, the rifting events ceased in the Neotethyan Ocean. At that time, the extensional regime was converted to compression.

According to Pearce, Lippard & Roberts (1984), Jones, Robertson & Cann (1991), Robertson (1994), Parlak & Delaloye (1999) and Andrew & Robertson (2002), continuous convergence induced a N-dipping subduction in the Neotethyan Ocean and it developed arc-related or supra-subduction zone ophiolites in the eastern Mediterranean region (Fig. 8a). Recent studies show that the Antalya ophiolite was also generated in a supra-subduction zone setting (Robertson, 2000; Bağcı *et al.* 2002).

The amphibolites display three different geochemical affinities: MORB, IAT and OIB (Çelik & Delaloye, 2003). Protoliths of IAT-type amphibolites could originate from the supra-subduction type ophiolites. OIB- and MORB-like amphibolites were generated from the ocean island and old subducted slab respectively (Fig. 8b).

Finally, all units of the Neotethyan Ocean were obducted onto the Tauride carbonate platform during Late Cretaceous to Palaeocene times (Fig. 8c).

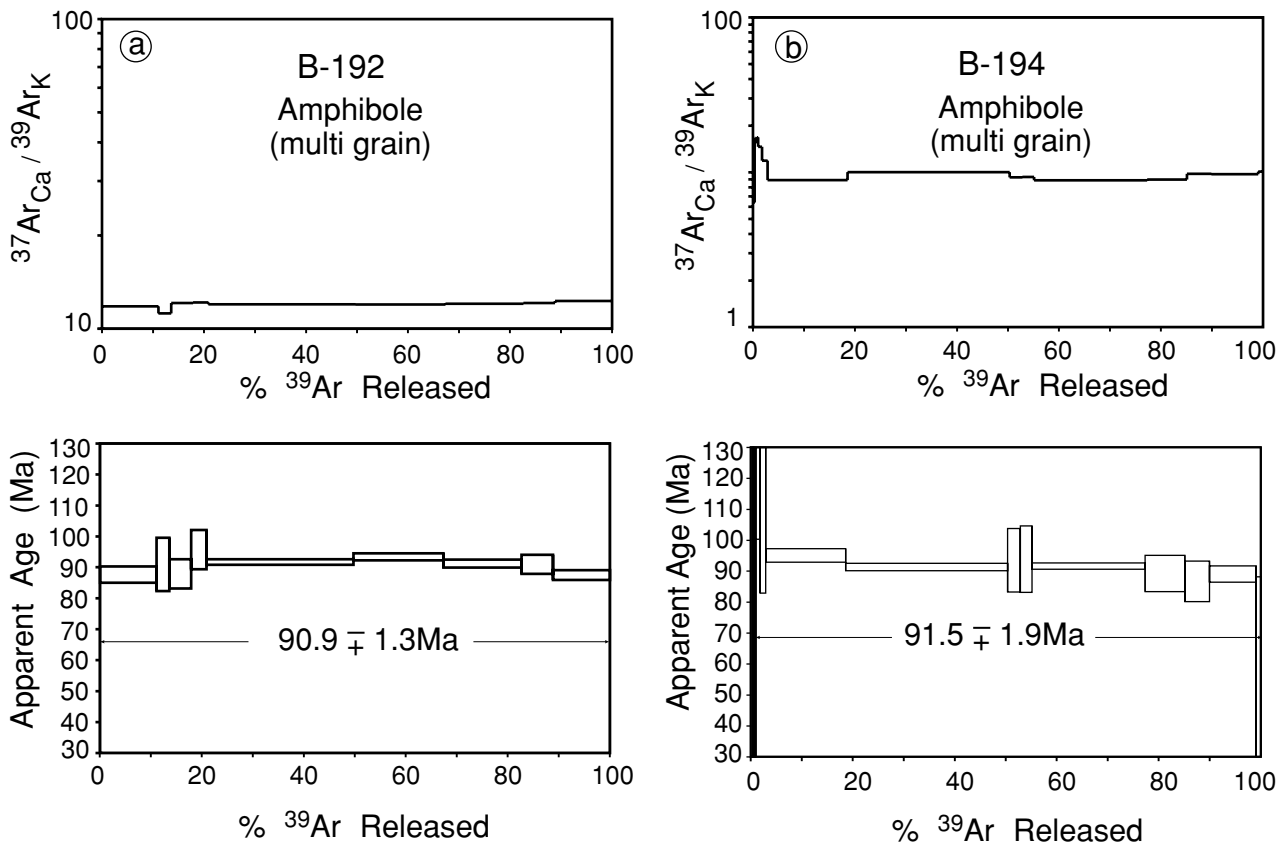


Figure 6. ^{40}Ar - ^{39}Ar ages and $^{37}\text{Ar}_{\text{Ca}}$ - $^{39}\text{Ar}_{\text{K}}$ ratio spectra for hornblende (a, b) from amphibolites of the Beyşehir ophiolite.

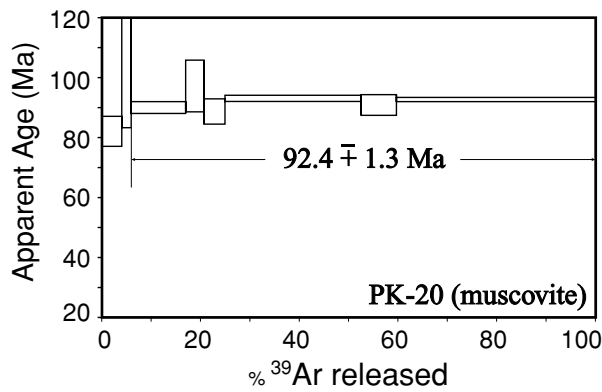


Figure 7. ^{40}Ar - ^{39}Ar age for white mica from mica schist of the Pozantı-Karsanti ophiolite.

6. Conclusions

Southern Turkey is a good region to study reconstruction of ophiolite emplacement along the Alpine-Himalayan orogenic belt. ^{40}Ar - ^{39}Ar measurements from the metamorphic sole rocks of Lycian, Antalya and Beyşehir ophiolites are the first precise ages indicating intra-oceanic thrusting and the cooling age history during the closure of the Neotethyan Ocean.

The ^{40}Ar - ^{39}Ar data display concordant plateau ages for different rocks from the same units. Metamorphic and cooling age of the amphibolites from the

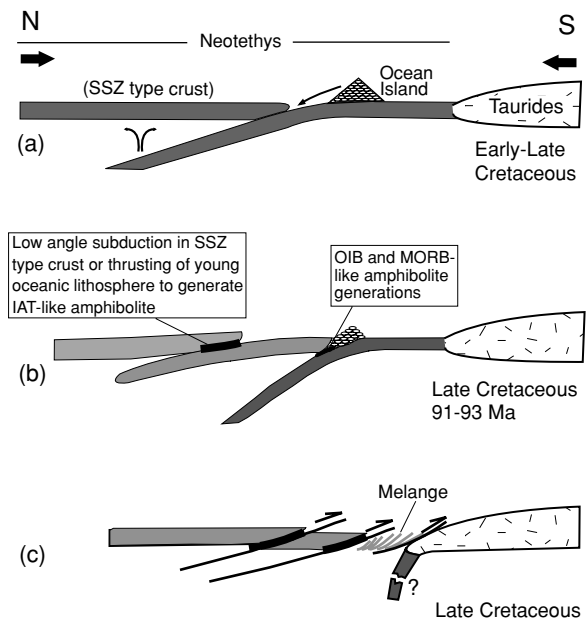


Figure 8. Tectonic diagram illustrating a double subduction model for the generation of the metamorphic sole rocks of the Tauride Belt Ophiolites.

five ophiolitic units of Köyceğiz, Yeşilova, Pozantı-Karsanti, Beyşehir and Antalya, extended over a wide area, range from 91 to 93 Ma. When both amphibole and white micas are analysed, the plateau ages are

concordant, indicating a fast cooling history. Accordingly, exhumation of the metamorphic sole rocks along the Tauride Belt Ophiolites was started in the oceanic environment after 93 Ma.

The metamorphic temperature in the sole rocks from Köyceğiz was approximately 550 °C. It corresponds to closure temperature of amphibole in the ^{40}Ar – ^{39}Ar system and therefore 93.1 ± 0.6 Ma could be interpreted as the metamorphic age of the amphibolites.

The hornblende plateau ages from the amphibolites of Köyceğiz (93.1 ± 0.9 Ma and 93.0 ± 0.9 Ma) are equivalent to those of Antalya (93.0 ± 1.0 and 93.8 ± 1.7 Ma), indicating that they were metamorphosed simultaneously in the Neotethyan Ocean.

Acknowledgements. The research presented in this paper was funded by the Swiss National Research Foundation through the projects (20-52294.97) and (20-058786.99). We thank Drs I. Yolcubal, E. Aldanmaz and Ö. F. Gürer for constructive suggestions. Helpful reviews of the manuscript were received from Dr V. Höck, Dr D. M. Pyle and an anonymous referee.

References

- ANDREW, T. & ROBERTSON, A. H. F. 2002. The Beyşehir-Hoyran-Hadim (B-H-H) Nappes: Mesozoic marginal and oceanic units of the Northern Neotethys in Southern Turkey. *Journal of the Geological Society, London* **59**, 529–43.
- BAĞCI, U., PARLAK, O., HÖCK, V. & DELALOYE, M. 2002. Suprasubduction origin of the Antalya Ophiolite (Southern Turkey): Deduced from the Mineral Chemistry of the Ultramafic-Mafic Cumulate Rocks. In *1st International Symposium of Istanbul Technical University, 16–18 May 2002*, Istanbul, Turkey, p. 140.
- ÇELİK, Ö. F. 2002. Geochemical, Petrological and Geochronological Observations on the Metamorphic Rocks of the Tauride Belt Ophiolites (S. Turkey). *Terre & Environment* **39**, Université de Genève, 257 pp. (published Ph.D. thesis).
- ÇELİK, Ö. F. & DELALOYE, M. F. 2002. New ^{40}Ar – ^{39}Ar and K–Ar age implications and geochemical constraints on metamorphic rocks of the Tauride Belt Ophiolites (Southern Turkey). *Geochimica et Cosmochimica Acta*, **66** (15A), A125 Supplement.
- ÇELİK, Ö. F. & DELALOYE, M. F. 2003. Origin of metamorphic soles and their post-kinematic mafic dyke swarms in the Antalya and Lycian ophiolites, SW Turkey. *Geological Journal* **38**, 235–56.
- ÇELİK, Ö. F. & DELALOYE, M. F. 2004. Mineral chemistry and P–T conditions of metamorphic sole rocks from the Lycian and the Antalya ophiolites, western Taurides (SW Turkey). In *Proceedings of 5th International Symposium on Eastern Mediterranean Geology, 14–20 April 2004* (eds A. A. Chatzipetros and S. B. Pavlides), p. 241. Thessaloniki, Greece.
- ÇELİK, Ö. F. & DELALOYE, M. F. 2006. Characteristics of ophiolite-related metamorphic rocks in the Beyşehir ophiolitic mélange (Central Taurides, Turkey), deduced from whole rock and mineral chemistry. *Journal of Asian Earth Sciences* **26**, doi: 10.1016/j.jseas.2004.10.008, in press.
- COLLINS, A. S. & ROBERTSON, A. H. F. 1997. Lycian melange, southwestern Turkey: An emplaced Late Cretaceous accretionary complex. *Geology* **25**, 255–8.
- COLLINS, A. S. & ROBERTSON, A. H. F. 1998. Processes of Late Cretaceous to Late Miocene episodic thrust-sheet translation in the Lycian Taurides, SW Turkey. *Journal of the Geological Society, London* **155**, 759–72.
- COLLINS, A. S. & ROBERTSON, A. H. F. 2003. Kinematic evidence for Late Mesozoic–Miocene emplacement of the Lycian Allochthon over the western Anatolide Belt, SW Turkey. *Geological Journal* **38**, 295–310.
- DİLEK, Y. & MOORES, E. M. 1990. Regional tectonics of the Eastern Mediterranean ophiolites. In *Ophiolites – oceanic crustal analogues: Proceedings of Troodos ophiolite symposium – 1987* (eds J. Malpas, E. Moores, A. Panayiotou and C. Xenophontos), pp. 295–309. Geological Survey, Cyprus.
- DİLEK, Y., THY, P., HACKER, B. & GRUNDTVIG, S. 1999. Structure and petrology of Tauride ophiolites and mafic dyke intrusions (Turkey): implications for the Neotethyan ocean. *Geological Society of America Bulletin* **111**, 1192–1216.
- GRAHAM, M. C. & POWELL, R. 1984. A garnet-hornblende geothermometer: calibration, testing, and application to the Pelona Schist, Southern California. *Journal of Metamorphic Geology* **2**, 13–31.
- HANSON, G. N. & GAST, P. W. 1967. Kinetic studies in contact metamorphic zones. *Geochimica et Cosmochimica Acta* **31**, 1119–53.
- HARRISON, T. M. 1981. Diffusion of ^{40}Ar in hornblende. *Contributions to Mineralogy and Petrology* **78**, 324–31.
- HOLLAND, T. J. B. & BLUNDY, J. D. 1994. Non-Ideal interactions in calcic amphiboles and their bearing on amphibole–plagioclase thermometry. *Contributions to Mineralogy and Petrology* **116**, 433–47.
- JONES, G., ROBERTSON, A. H. F. & CANN, J. R. 1991. Genesis and emplacement of the supra-subduction zone Pindos ophiolite, northwestern Greece. In *Ophiolite Genesis and Evolution of the Oceanic Lithosphere* (eds T. J. Peters, A. Nicolas and R. G. Coleman), pp. 771–9. Dordrecht: Kluwer Academic Publishing.
- JUTEAU, T. 1980. Ophiolites of Turkey. *Ofioliti* **2**, 199–235.
- LEAKE, B. E., WOOLLEY, A. R., ARPS, C. E. S., BIRCH, W. D., GILBERT, M. C., GRICE, J. D., HAWTHORNE, F. C., KATO, A., KISCH, H. J., KRIVOVICHEV, V. G., LINTHOUT, K., LAIRD, J., MANDARINO, J., MARESCH, W. V., NICKEL, E. H., ROCK, N. M. S., SCHUMACHER, J. C., SMITH, D. C., STEPHENSON, N. C. N., UNGARETTI, L., WHITTAKER, E. J. W. & YOUZHI, G. 1997. Nomenclature of amphiboles: Report of the subcommittee on amphiboles of the International Mineralogical Association, commission on new minerals and mineral names. *American Mineralogist* **82**, 1019–37.
- ÖZGÜL, N., 1976. Torosların bazı temel jeoloji özellikleri. *Geological Society of Turkey Bulletin* **19**, 65–78.
- PARLAK, O. 1996. Geochemistry and geochronology of the Mersin ophiolite within the eastern Mediterranean tectonic frame (southern Turkey). *Terre & Environment* **6**, Université de Genève, 242 pp. (published Ph.D. thesis).
- PARLAK, O. & DELALOYE, M. 1999. Precise ^{40}Ar – ^{39}Ar ages from the metamorphic sole of the Mersin ophiolite (Southern Turkey). *Tectonophysics* **301**, 145–58.
- PARLAK, O., DELALOYE, M. & BİNGÖL, E. 1995. Origin of sub-ophiolitic metamorphic rocks beneath the Mersin ophiolite, Southern Turkey. *Ofioliti* **20**, 97–110.

- PARLAK, O. & ROBERTSON, A. H. F. 2004. The ophiolite-related Mersin Melange, southern Turkey: its role in the tectonic-sedimentary setting of Tethys in the Eastern Mediterranean region. *Geological Magazine* **141**, 257–86.
- PEARCE, J. A., LIPPARD, S. J. & ROBERTS, S. 1984. Characteristics and tectonic significance of supra-subduction zone ophiolites. In *Marginal Basin Geology* (eds B. P. Kokelaar and M. F. Howells), pp. 77–89. Geological Society of London, Special Publication no. 16.
- POLAT, A. & CASEY, J. F. 1995. A structural record of the emplacement of the Pozanti-Karsanti ophiolite onto the Mendere-Taurus block in Late Cretaceous, eastern Taurides, Turkey. *Journal of Structural Geology* **17**, 1673–88.
- RENNE, P. R., SWISHER, C. C., DEINO, A. L., KARNER, D. B., OWENS, T. L. & DEPAOLO, D. J. 1998. Intercalibration of standards, absolute ages and uncertainties in $^{40}\text{Ar}/^{39}\text{Ar}$ dating. *Chemical Geology* **145**, 117–52.
- RICOU, L. E., ARGRIADIS, I. & MARCOUX, J. 1975. L'axe calcaire du Taurus, une alignement de fenêtres arabo-africaines sous des nappes radiolaritiques, ophiolitiques et métamorphiques. *Bulletin de la Société géologique de France* **17**, 1024–43.
- ROBERTSON, A. H. F. 1994. Role of tectonic facies concept in orogenic analysis and its application to Tethys in the Eastern Mediterranean region. *Earth Science Review* **37**, 139–213.
- ROBERTSON, A. H. F. & WOODCOCK, N. H. 1980. Mamonia Complex, southwest Cyprus: Evolution and emplacement of a Mesozoic continental margin. *Geological Society of America Bulletin* **90**, 651–65.
- ROBERTSON, A. H. F. 2000. Mesozoic–Tertiary tectonic–sedimentary evolution of a south Tethyan oceanic basin and its margins in southern Turkey. In *Tectonics and Magmatism in Turkey and Surrounding Area* (eds E. Bozkurt, J. A. Winchester and J. D. A. Piper), pp. 43–82. Geological Society of London, Special Publication no. 173.
- ŞENGÖR, A. M. C. & YILMAZ, Y. 1981. Tethyan evolution of Turkey: a plate tectonic approach. *Tectonophysics* **75**, 181–241.
- SMITH, A. G., HURLEY, A. M. & BRIDEN, J. C. 1981. *Phanerozoic palaeocontinental maps*. Cambridge: Cambridge University Press.
- STEIGER, R. H. & JAEGER, E. 1977. Subcommittee on Geochronology: convention on the use of decay constants in geo- and cosmochronology. *Earth and Planetary Science Letters* **55**, 359–62.
- THUIZAT, R., WHITECHURCH, H., MONTIGNY, R. & JUTEAU, T. 1981. K–Ar dating of some infra-ophiolitic metamorphic soles from the eastern Mediterranean: New evidence for oceanic thrusting before obduction. *Earth and Planetary Science Letters* **52**, 302–10.
- WHITECHURCH, H., JUTEAU, T. & MONTIGNY, R. 1984. Role of the eastern Mediterranean ophiolites (Turkey, Syria, Cyprus) in the history of the Neotethys. In *The geological evolution of the eastern Mediterranean* (eds J. E. Dixon and A. H. F. Robertson), pp. 301–17. Geological Society of London, Special Publication no. 17.
- YILMAZ, P. O. & MAXWELL, J. C. 1982. K–Ar investigations from the Antalya Complex ophiolites, SW Turkey. *Ophioliti* **7**, 527–38.
- YILMAZ, P. O. & MAXWELL, J. C. 1984. An example of an obduction mélange: the Alakır Çay unit, Antalya Complex, southwest Turkey. In *Mélanges: Their Nature, Origin, and Significance* (eds L. A. Raymond), pp. 139–52. Geological Society of America, Special Publication no. 198.